

Study of low-energy magnetic excitations in single-crystalline CeIn_3 by inelastic neutron scattering

W. Knafo[†], S. Raymond[†], B. Fåk[‡], G. Lapertot[†], P.C. Canfield[§] and J. Flouquet[†]

[†] CEA-Grenoble, DRFMC/SPSMS/MDN, 38054 Grenoble Cedex, France

[‡] ISIS Facility, Rutherford Appleton Laboratory, Chilton, Didcot, Oxon OX11 0QX, England

[§] Ames Laboratory, Iowa State University, Ames Iowa 50011, USA

Abstract.

Inelastic neutron scattering experiments were performed on single crystals of the heavy-fermion compound CeIn_3 for temperatures below and above the Néel temperature, T_N . In the antiferromagnetically ordered phase, well-defined spin-wave excitations with a bandwidth of 2 meV are observed. The spin waves coexist with quasielastic (QE) Kondo-type spin-fluctuations and broadened crystal-field (CF) excitations below T_N . Above T_N , only the QE and CF excitations persist, with a weak temperature dependence.

PACS numbers: 71.27.+a, 75.40.Gb, 78.70.Nx

Submitted to: *Institute of Physics Publishing*

Printed: 7 February 2020

1. Introduction

A quantum critical point (QCP) occurs in the heavy fermion (HF) compound CeIn_3 under a hydrostatic pressure of $P_C = 25$ kbar. This corresponds to a transition at $T = 0$ K from a magnetically ordered to a disordered state. It was found that at least up to 23 kbar the ground state is antiferromagnetically ordered with a propagation vector $\mathbf{k} = (1/2, 1/2, 1/2)$. At ambient pressure the Néel temperature is $T_N = 10.1$ K and the staggered magnetization is $m_0 = 0.5 \mu_B$ [1, 2]. CeIn_3 becomes superconducting below $T_C = 200$ mK in the vicinity of P_C [3, 4]. More generally, the appearance of unconventional superconductivity around P_C in HF systems is supposed to be related to the enhancement of magnetic fluctuations when $T_N \simeq 0$.

CeIn_3 crystallizes in the cubic AuCu_3 structure, and hence the magnetic fluctuations are expected to be three-dimensional (3D). This is confirmed by resistivity measurements, which show a $\Delta\rho = T^{3/2}$ non Fermi liquid (NFL) behavior at the critical

pressure, as expected for 3D fluctuations in spin-fluctuation theories [5, 6]. Recently, a new family of HF compounds was discovered [7], $Ce_m T_n In_{3m+2n}$, which is composed of alternating layers of $CeIn_3$ and TIn_2 stacked along the c -direction with $T = Ir, Rh,$ or Co . Their main interest arises from the layered structure that is thought to induce 2D fluctuations that would enhance the superconductivity more than 3D fluctuations near T_C [8]. Indeed, $CeCoIn_5$ has a superconducting state at ambient pressure below $T_C = 2.3$ K, the highest T_C observed up to now in HF systems [9]. These recent results motivated us to reinvestigate the common brick of these quasi 2D compounds: the 3D heavy fermion $CeIn_3$.

Previous inelastic neutron scattering (INS) studies on powder samples of $CeIn_3$ [10, 11] showed the existence of a crystal field (CF) excitation at $\Delta_{CF} \simeq 12$ meV with a large broadening ascribed to the Kondo effect. In this work, we present new INS measurements on single crystals, which due to new flux growing methods are now sufficiently large for such studies. These measurements show the existence of well-defined spin-wave excitations in the magnetically ordered phase, which coexist with quasielastic (QE) Kondo-type spin-fluctuations and the previously observed broadened crystal-field excitations.

2. Experimental details

The single crystals used in this study were grown by the self flux method [12]. A first set of neutron scattering measurements was carried out on the time-of-flight chopper spectrometer MARI at ISIS, using incident energies of 22 and 60.3 meV. The corresponding energy resolution was approximately 2 and 5 meV, respectively. Because of the strong neutron absorption cross-section of In, the single crystals were cut to a thickness of 2 mm and used in transmission geometry. A total of 30 crystals with total weight of 13 g were aligned and glued to a thin aluminium plate, which was mounted in a closed-cycle refrigerator. The mosaicity of the assembly was approximately 6° . Measurements were performed in the (hhl) plane, with an angle between the incident wavevector and the [001] direction of 2.5 and 30° .

A second set of neutron scattering measurements was made on the triple-axis spectrometer IN22 at the ILL (Grenoble, France). Pyrolytic graphite was used for the vertically focusing monochromator and the horizontally focusing analyzer. A PG filter in the scattered beam was used to suppress higher order contamination, and final neutron energies of 8.05 and 14.7 meV were used, giving an energy resolution of 0.5 and 1.0 meV, respectively. Two thin plates of the assembly used on MARI were aligned on an aluminum support and mounted in a helium flow "orange" cryostat. The total mass of the sample was about 1 g and the mosaicity 0.5° . The (hhl) scattering plane was investigated.

3. Results

3.1. Crystal-field excitation and quasielastic line

For the two crystals orientations used on MARI and at temperatures of $T = 5, 15$ and 150 K, we recorded (\mathbf{Q}, E) intensity maps for $0 < Q < 10 \text{ \AA}^{-1}$ and $E < 30$ meV, where \mathbf{Q} is the wavevector transfer and E is the energy transfer. Despite strong phonon contamination from both the $CeIn_3$ sample and the Al support, we observed an excitation around 12 meV which was independent of the crystal orientation and whose intensity decreased with Q . The temperature dependence of the 12 meV excitation obtained for $Q < 2 \text{ \AA}^{-1}$ is shown in figure 1. The excitation shows only a very slight softening and broadening as the temperature goes from the ordered state at $T = 5$ K to the paramagnetic state at $T = 15$ K. At much higher temperatures, $T = 150$ K, the excitation is partly suppressed. Figure 2 shows the wavevector dependence of the excitation spectrum at $T = 5$ K. The peak at 12 meV observed at low Q (integration over $0 < Q < 2 \text{ \AA}^{-1}$) disappears at higher wave vectors (integration over $7.5 < Q < 7.8 \text{ \AA}^{-1}$), reflecting its magnetic nature. The contribution around 20 meV, seen only at high Q 's, is due to phonons. The Q and T dependence of the 12 meV excitation, as illustrated in Figs. 1 and 2, clearly show its magnetic origin, and corresponds to the CF excitation observed in powder samples by Lawrence et al. [10] and Murani et al. [11].

The cubic environment of Ce^{3+} in $CeIn_3$ can be treated in terms of Stevens operators by the following CF Hamiltonian: $H_{CF} = B_4(O_4^0 + 5O_4^4)$ [13]. This Hamiltonian splits the $J = 5/2$ spin-orbit level of Ce^{3+} into a Γ_8 quartet and a Γ_7 doublet. In the case of $CeIn_3$, susceptibility measurements indicates that $B_4 > 0$ [14], implying that the ground state is Γ_7 . This has been confirmed by polarized neutron scattering measurements, which also reveals an admixture of Γ_8 to the ground state Γ_7 in the ordered phase [15]. The excitation observed here at 12 meV corresponds then to the $\Gamma_7 \rightarrow \Gamma_8$ excitation.

In addition to the 12 meV CF excitation, it is clear from the data that there is an additional quasielastic (QE) component to the scattering. The low- Q data at $T = 5$ K were therefore analyzed using three components: an incoherent elastic peak, a quasielastic spin-fluctuation contribution, and a crystal-field excitation. Since the different contributions partly overlap, we fixed the width (half width at half maximum, HWHM) Γ_{QE} of the QE contribution to $k_B T_K = 0.86$ meV where $T_K = 10$ K is the Kondo temperature. The results of the analysis at $T = 5$ K give a crystal-field splitting of $\Delta_{CF} = 10.6 \pm 0.2$ meV and a broadening of the CF levels (HWHM) of $\Gamma_{CF} = 5.7 \pm 0.2$ meV. No significant difference in the values of the CF excitations were found for the different orientations of the crystal. At $T = 15$ K, the resulting CF splitting is $\Delta_{CF} = 9.4 \pm 0.2$ meV and its width is $\Gamma_{CF} = 6.0 \pm 0.2$ meV. The slight softening observed of Δ_{CF} is related to the splitting of the CF levels below T_N .

3.2. Spin wave

The dispersive mode that appears below T_N was first observed using the MARI chopper spectrometer. Because of the 3D character of this mode, the study of its dispersion was continued using the IN22 triple-axis spectrometer. Energy scans up to 6 meV energy transfer were measured for different values of the wavevector transfer \mathbf{Q} . Figure 3 shows spectra of CeIn₃ at $\mathbf{Q} = (-1.2, -1.2, 0.5)$ for $T = 1.5$ and 15 K. This corresponds to the reduced wavevector $\mathbf{q} = \mathbf{Q} - \tau - \mathbf{k} = (0.3, 0.3, 0)$, where $\tau = (-1, -1, 1)$ is a reciprocal lattice vector and $\mathbf{k} = (-1/2, -1/2, -1/2)$ is a magnetic propagation vector (wavevectors are expressed in reciprocal lattice unit with 1 r.l.u. = $2\pi/a$, where $a = 4.689 \text{ \AA}$ is the lattice parameter). Figure 3 clearly shows that the excitation present at $T < T_N$ disappears for $T > T_N$. For each wavevector \mathbf{q} , the excitation was fitted by a Gaussian whose width corresponds to the instrumental resolution. The strong dispersion of this excitation in the three main directions of the crystal is shown in figure 4. Since the direction of the ordered moment in CeIn₃ is unknown and our sample is in a multidomain state, it is not possible to determine the polarization of the excitation; it will be assumed to be transverse as for a conventional spin wave.

Supposing that the CF energy is of the same order as the exchange interaction, it seems appropriate to treat the spin wave using the so-called molecular-field random-phase approximation [16]. Writing the exchange Hamiltonian as

$$H_{ex} = - \sum_{i,j} I_{ij} \mathbf{J}_i \mathbf{J}_j \quad (1)$$

gives the general dispersion relation

$$E(\mathbf{q}) = \{[\Delta - M^2 I(\mathbf{q})][\Delta - M^2 I(\mathbf{q} + \mathbf{k})]\}^{1/2}, \quad (2)$$

where \mathbf{k} is the propagation vector of the ordered state, $I(\mathbf{q})$ the Fourier transform of the exchange interaction I_{ij} , and Δ the splitting of the Γ_7 doublet into $\Gamma_{7,1}$ and $\Gamma_{7,2}$ due to the molecular and anisotropy fields. The transition matrix element between the ground state $\Gamma_{7,1}$ and the first excited state $\Gamma_{7,2}$ is given by $M^2 = |\langle \Gamma_{7,2} | J^\alpha | \Gamma_{7,1} \rangle|^2$ ($\alpha = +$ or $-$). Considering only the nearest neighbor exchange I_1 [along (1,0,0)] and the next nearest neighbor exchange I_2 [along (1,1,0)], the exchange interaction is

$$\begin{aligned} I(\mathbf{q}) = & 2I_1 [\cos(2\pi q_x) + \cos(2\pi q_y) + \cos(2\pi q_z)] \\ & + 2I_2 [\cos(2\pi(q_x - q_y)) + \cos(2\pi(q_y - q_z)) + \cos(2\pi(q_z - q_x)) \\ & + \cos(2\pi(q_x + q_y)) + \cos(2\pi(q_y + q_z)) + \cos(2\pi(q_z + q_x))]. \end{aligned} \quad (3)$$

In a two sub-lattice picture constituted of alternating (1,1,1) planes where the spins are up or down, I_1 would correspond to the antiferromagnetic exchange between spins from different sublattices and I_2 would correspond to the ferromagnetic exchange between spins from the same sublattice. A global fit to the dispersion curves of equation (2) is shown in figure 4. It gives the exchange terms $M^2 I_1 = -0.354 \pm 0.040$ meV and $M^2 I_2 = 0.028 \pm 0.013$ meV and the Γ_7 splitting $\Delta = 2.812 \pm 0.480$ meV. The corresponding spin-wave gap is : $\delta = E(\mathbf{0}) = 1.28$ meV.

The exchange energy can be expressed by $E_{ex} = \frac{2J(J+1)}{3}I(\mathbf{0})$. Taking the wave functions of $\Gamma_{7,1}$ and $\Gamma_{7,2}$ when there is neither exchange nor distortion [17] gives us an approximated square transition matrix element $M^2 = 2.78$ thus $I(\mathbf{0}) = -0.64 \pm 0.18$ meV. With $J = 5/2$, we obtain $E_{ex} \simeq 3.71$ meV. The ratio $\Delta_{CF}/|E_{ex}| \simeq 3$ permits then to conclude that the CF energy is of the same order than the exchange interaction that justifies the treatment of the spin wave using the molecular-field random-phase approximation.

4. Discussion

4.1. Kondo temperature

We have analyzed the Q-independent excitations using two contributions, one corresponding to quasielastic scattering and the other to a crystal-field transition. Since these excitations overlap with each other and with the incoherent peak (see figure 2), the energy, width, and weight of the different contributions extracted from the data depend on the model used for the fitting. This is illustrated by the scatter in the estimates of Δ_{CF} , Γ_{CF} , and Γ_{QE} found in the literature [10, 11, 18, 19]. At low temperatures, the QE excitation corresponds to the spin fluctuations of the Γ_7 electronic level, which are attributed to the Kondo effect. Its width (HWHM) Γ_{QE} corresponds to the Kondo temperature. A Kondo temperature of $T_K = 10$ K at a pressure of $P = 19$ kbar was obtained in ^{115}In -NQR measurements by Kawasaki et al. [20]. It is likely that below this pressure the anomaly at T_N in the $1/T_1$ temperature variation masks the T_K anomaly. We assume therefore that T_K has a very slight variation for pressures below $P = 19$ kbar, so that it is only slightly smaller than 10 K at ambient pressure. Resistivity measurements give a Kondo scattering maximum at $T_M \simeq 50$ K [4], which corresponds to the high Kondo temperature $T_K^h = \sqrt[3]{T_K(\Delta_{CF}/k_B)^2}$ [21]. INS gives $\Delta_{CF} = 10.6$ meV which with $T_K^h = 50$ K leads to $T_K \simeq 8$ K. It is then reasonable to approximate the Kondo temperature by $T_K \simeq 10$ K in $CeIn_3$ at ambient pressure. For the INS measurement carried out at $T = 5$ K $< T_K$, we choose consequently to fix the QE width to $\Gamma_{QE} = k_B T_K = 0.86$ meV. The fact that $\Gamma_{CF} = 5.7$ meV is relatively large compared to $\Gamma_{QE} = 0.86$ meV is due to the larger spin fluctuations associated with the Γ_8 first excited level. In fact, the CF transition $\Gamma_7 \rightarrow \Gamma_8$ has a width corresponding to the convolution of the Γ_7 and Γ_8 widths $\Gamma_{QE}^{\Gamma_7} = \Gamma_{QE}$ and $\Gamma_{QE}^{\Gamma_8}$. We can approximate $\Gamma_{CF} \simeq \Gamma_{QE}^{\Gamma_7} + \Gamma_{QE}^{\Gamma_8}$ and thus estimate that $\Gamma_{QE}^{\Gamma_8} \simeq \Gamma_{CF} - \Gamma_{QE} = 4.84$ meV, which is effectively 5 times larger than Γ_{QE} .

4.2. Anisotropy

Even if the CF level is broad, it seems that the propagating spin waves can be described by considering Γ_7 as an "isolated" doublet split by the anisotropy and exchange fields. Since this doublet originates from a sixfold degenerate $J = 5/2$ level, an anisotropy gap is expected in the spin-wave spectrum. We recall that in the isotropic case, the

spin-wave dispersion has no gap, since only the exchange is responsible for the splitting Δ .

The gap δ of the spin wave excitation corresponds to its minimum energy that is obtained at $\mathbf{q} = (0,0,0)$. Since this excitation overlaps with the incoherent elastic scattering that reflects the experimental resolution and with the quasielastic contribution of the spin fluctuations, the gap was not correctly obtained in the present neutron experiment. The given value of δ corresponds to the best fit to the data using the spin-wave model described above. An attempt to directly observe the gap using a smaller incident energy (and hence better resolution) on the cold triple-axis spectrometer IN12 (ILL) failed because of the strong indium absorption cross-section. A determination of the energy gap was also made by low-temperature specific-heat measurements which exhibited a spin wave contribution that leads to a gap $\delta = 0.69$ meV [22]. This suggests that the gap energy of 1.28 meV deduced from our INS measurements is somewhat overestimated.

The result of our spin-wave analysis is in good agreement with calculations made by Wang et al. for Ce^{3+} ions under cubic crystal field and effective exchange field [17]. They consider a molecular field along the c-axis, which can be approximated by $g\mu_B H_m = k_B T_N$, and calculate the level splitting as a function of $g\mu_B H_m/B_4$. Knowing that for $CeIn_3$ $T_N = 10.1$ K, $\Delta_{CF} = 10.6$ meV and hence $B_4 = 2.94 \cdot 10^{-2}$ meV ($\Delta_{CF} = 360 B_4$), we have $g\mu_B H_m = 8.71 \cdot 10^{-1}$ meV $\simeq 30 B_4$. For this value of $g\mu_B H_m/B_4$, Wang et al. calculate a Γ_7 splitting of about $40 B_4 \simeq 1.2$ meV. Although we suppose that in our case the molecular field is not along the c-axis (see below), we believe that Wang's calculations give the right order of the splitting Δ .

There are several indications for that the moments are not along the c-axis. If the CF alone imposes the easy magnetization axis, the positive sign of B_4 in the CF Hamiltonian implies that the moments are along the [1,1,1] direction in the ordered phase. This is also supported by nuclear quadrupolar resonance measurements [23]. Although it is difficult to determine the moment direction of a cubic compound by neutron diffraction, some recent measurements also suggest that the moments are not along the c-axis [22].

4.3. Comparison with $CePd_2Si_2$

$CeIn_3$ seems to have a behavior very similar to the HF compound $CePd_2Si_2$ which is antiferromagnetically ordered at ambient pressure and has the same kind of excitation spectrum with coexisting QE, CF, and spin-wave excitations [24]. The characteristic energies are very close and, moreover, unconventional superconductivity appears at a similar external pressure [3]. A summary of the characteristic physical quantities of those two compounds is given in Table 1. A focus on the few differences between those two compounds can be made as following. Firstly $CePd_2Si_2$ is tetragonal while $CeIn_3$ is cubic. Some characteristics such as the CF splitting or the susceptibility anisotropy can be directly linked to anisotropy effects that are resulting from those lattice structures.

Table 1. Characteristic physical quantities of $CeIn_3$ and $CePd_2Si_2$. Data are taken from [3], [4], [22], [24], [25], [26], [27], [28].

	$CeIn_3$	$CePd_2Si_2$
T_N	10.1 K	10 K
\mathbf{k}	(1/2,1/2,1/2)	(1/2,1/2,0)
m_0	0.50 μ_B	0.62 μ_B
δ	0.69 meV	0.83 meV
Bandwidth	~ 2 meV	~ 2 meV
θ_P	-50 K	-47 K *
T_K	10 K	10 K
Δ_{CF}	123 K	220 and 280 K
P_C	26.5 kbar	28.6 kbar
T_C	200 mK	430 mK
γ^{**}	130 $mJ.mol^{-1}.K^{-2}$	250 $mJ.mol^{-1}.K^{-2}$

* : DC susceptibility measurement along a-axis

** : $\gamma = C/T$ at low T

Then, the characteristic quantities T_C and γ are twice bigger in $CePd_2Si_2$ than in $CeIn_3$, that could traduce an enhancement of the spin fluctuations in the tetragonal $CePd_2Si_2$. As a supplement to the studies of quasi 2D $Ce_mT_nIn_{3m+2n}$ compounds where T_C can reach more than 2 K, an alternative way to study the influence of anisotropy in strongly correlated systems could consequently remain in a detailed comparison between cubic $CeIn_3$ and tetragonal $CePd_2Si_2$.

5. Conclusion

We have performed the first inelastic neutron scattering measurements on single crystals of $CeIn_3$. The combined use of time-of-flight and triple-axis spectrometers allowed us to study both local and dispersive low-energy excitations. We found the coexistence below T_N of a spin-wave with a quasielastic component and a crystal-field excitation. The CF levels are substantially broadened by Kondo-type spin fluctuations, which indicates the proximity to an intermediate valence state where the CF collapse. Despite the smearing of the CF levels, the observation of spin waves means that the ground state level in $CeIn_3$ is also relatively well-defined. The challenge is then to understand how these excitations evolve on going toward a QCP where the hierarchy between the Kondo effect and the RKKY coupling is reversed while the CF should be close to a collapse.

Acknowledgments

We acknowledge the help of K. Mony for sample preparation and X-ray characterization. We thank also A.P. Murani for many useful and stimulating discussions.

References

- [1] Morin P., Vettier C., Flouquet J., Konczykowski M., Lassailly Y., Mignot J.M. and Welp U. 1988 *J Low Temp Phys* **70** 377.
- [2] Benoit B., Boucherle J.X., Convert P., Flouquet J., Palleau J. and Schweizer J. 1980 *Solid State Comm.* **34** 293.
- [3] Mathur N.D., Grosche F.M., Julian S.R., Walker I.R., Freye D.M., Haselwimmer R.K.W. and Lonzarich G.G. 1998 *Nature* **394** 39.
- [4] Knebel G., Braithwaite D., Canfield P.C., Lapertot G., Flouquet J. 2001 *Phys. Rev. B* **65** 24425.
- [5] Millis A. 1993 *Phys. Rev. B* **48** 7183.
- [6] Moriya T. and Takimoto T. 1995 *J. Phys. Soc. Japan* **64** 960.
- [7] Thompson J.D., Movshovich R., Fisk Z., Bouquet F., Curro N.J., Fisher R.A., Hammel P.C., Hegger H., Hundley M.F., Jaime M., Pagliuso P.G., Petrovic C., Phillips N.E. and Sarrao J.L. 2001 *J. Magn. Magn. Mat.* **226-230** 5.
- [8] Monthoux P. and Lonzarich G.G. 2001 *Phys. Rev. B* **63** 054529.
- [9] Petrovic C., Pagliuso P.G., Hundley M.F., Movshovich R., Sarrao J.L., Thompson J.D., Fisk Z., and Monthoux P. 2001 *J. Phys.: Condens. Matter* **13** L337.
- [10] Lawrence J.M. and Shapiro S.M. 1980 *Phys. Rev. B* **22** 4379.
- [11] Murani A.P., Taylor A.D., Osborn R. and Bowden Z.A. 1993 *Phys. Rev. B* **48** 10606.
- [12] Canfield P.C. and Fisk Z. 1992 *Philos. Mag. B* **65** 1117.
- [13] Lea K.R., Leask M.J.M., Wolf W.P. 1962 *J. Phys. Chem. Solids* **23** 1381.
- [14] Buschow K.H.J., De Wijn H.W. and Van Diepen A.M. 1969 *J. Chem. Phys.* **50** 137.
- [15] Boucherle J.X., Flouquet J., Lassailly Y., Palleau J. and Schweizer J. 1983 *J. Magn. Magn. Mat.* **31-34** 409.
- [16] Buyers W.J.L., Holden T.M. and Perreault A. 1975 *Phys. Rev. B* **11** 266.
- [17] Wang Y.L. and Cooper B.R. 1970 *Phys. Rev. B* **2** 2607.
- [18] Groß W., Knorr K., Murani A.P. and Buschow K.H.J. 1980 *Z. Phys. B* **37** 123.
- [19] Lassailly Y., Burke S.K. and Flouquet J. 1985 *J. Phys. C* **18** 5737.
- [20] Kawasaki S., Mito T., Zheng G.-q., Thessieu C., Kawasaki Y., Ishida K., Kitaoka Y., Muramatsu T., Kobayashi T.C., Aoki D., Araki S., Haga Y., Settai R. and Ōnuki Y. 2001 *Phys. Rev. B* **65** 020504.
- [21] Hanzawa K., Yamada K. and Yosida K. 1985 *J. Magn. Magn. Mat.* **47-48** 357.
- [22] Knafo W. et al., *in preparation*
- [23] Kohori Y., Kohara T., Yamato Y., Tomka G. and Riedi P.C. 2000 *Physica B* **281-282** 12.
- [24] Van Dijk N.H., Fåk B., Charvolin T., Lejay P. and Mignot J.M. 2000 *Phys. Rev. B* **61** 8922.
- [25] Grier B.H., Lawrence J.M., Murgai V. and Parks R.D. 1984 *Phys. Rev. B* **29** 2664.
- [26] Demuer A., Jaccard D., Sheikin I., Raymond S., Salce B., Thomasson J., Braithwaite D. and Flouquet J. 2001 *J. Phys. Condens. Matter* **13** 9335.
- [27] Steeman R.A., Mason T.E., Lin H., Buyers W.J.L., Menovsky A.A., Collins M.F., Frikkee E., Nieuwenhuys G.J. and Mydosh J.A. 1990 *J. Appl. Phys.* **67** 5203.
- [28] Grosche F.M., Julian F.R., Mathur N.D. and Lonzarich G.G. 1996 *Physica B* **223-224** 50.

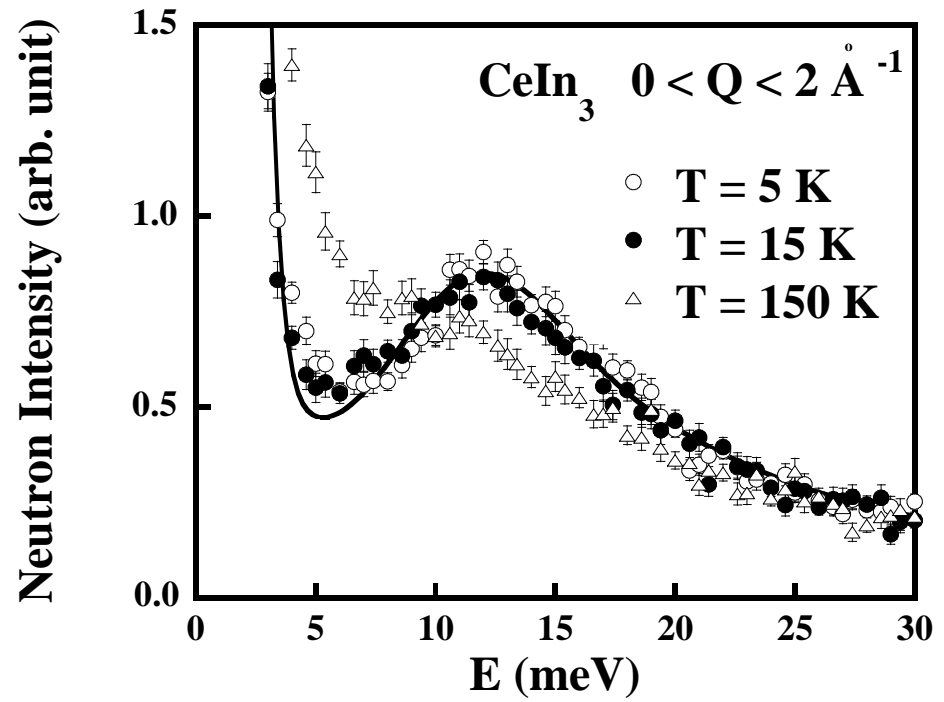


Figure 1. Energy scans at different temperatures obtained on MARI spectrometer using an incident energy of 60.3 meV and integrating over Q values between 0 and 2 \AA^{-1} . The solid line shows the total fit for $T = 5 \text{ K}$.

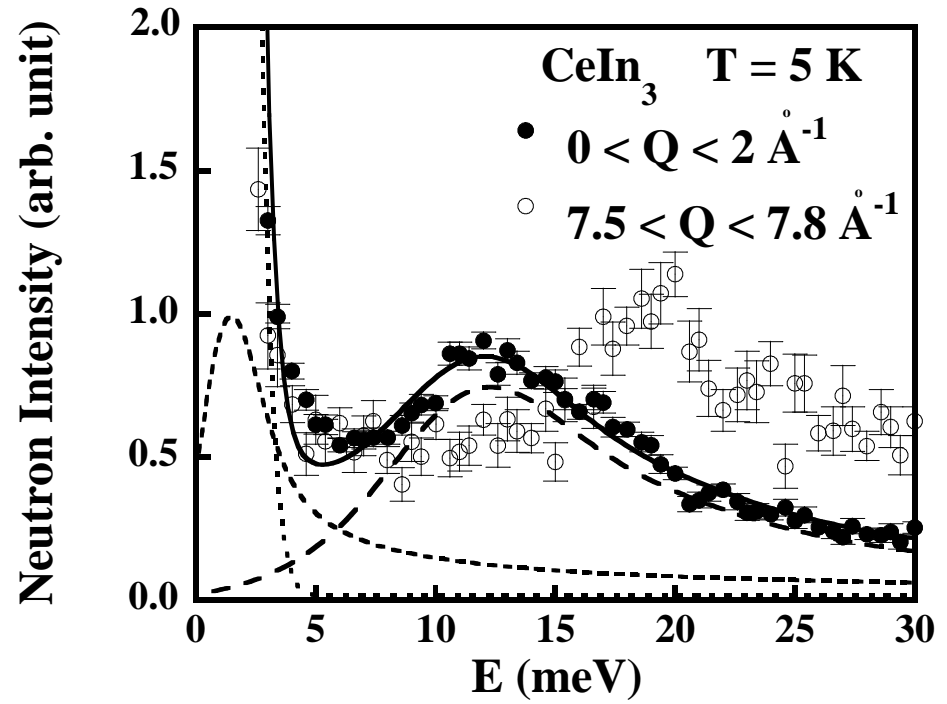


Figure 2. Energy scans at different wavevectors obtained on the MARI spectrometer using an incident energy of 60.3 meV at $T = 5$ K. The long dashed, short dashed, and dotted lines show the CF, QE, and incoherent contributions of the small Q spectrum, respectively, while the solid line shows the total fit.

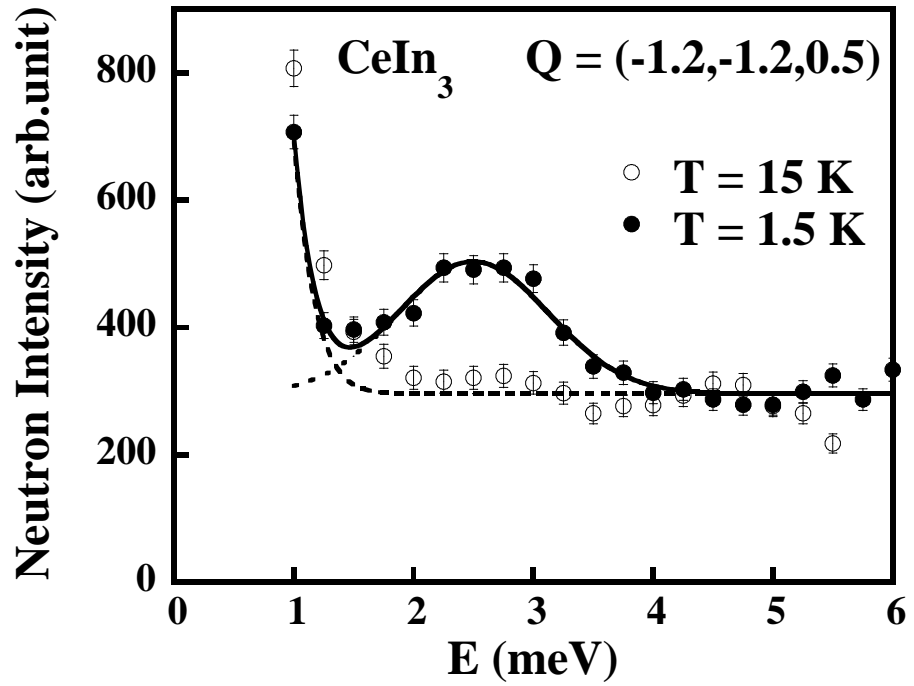


Figure 3. Energy scans at $\mathbf{Q} = (-1.2, -1.2, 0.5)$ for temperatures of $T = 1.5$ and 15 K obtained on the IN22 spectrometer using a final energy of 14.7 meV.

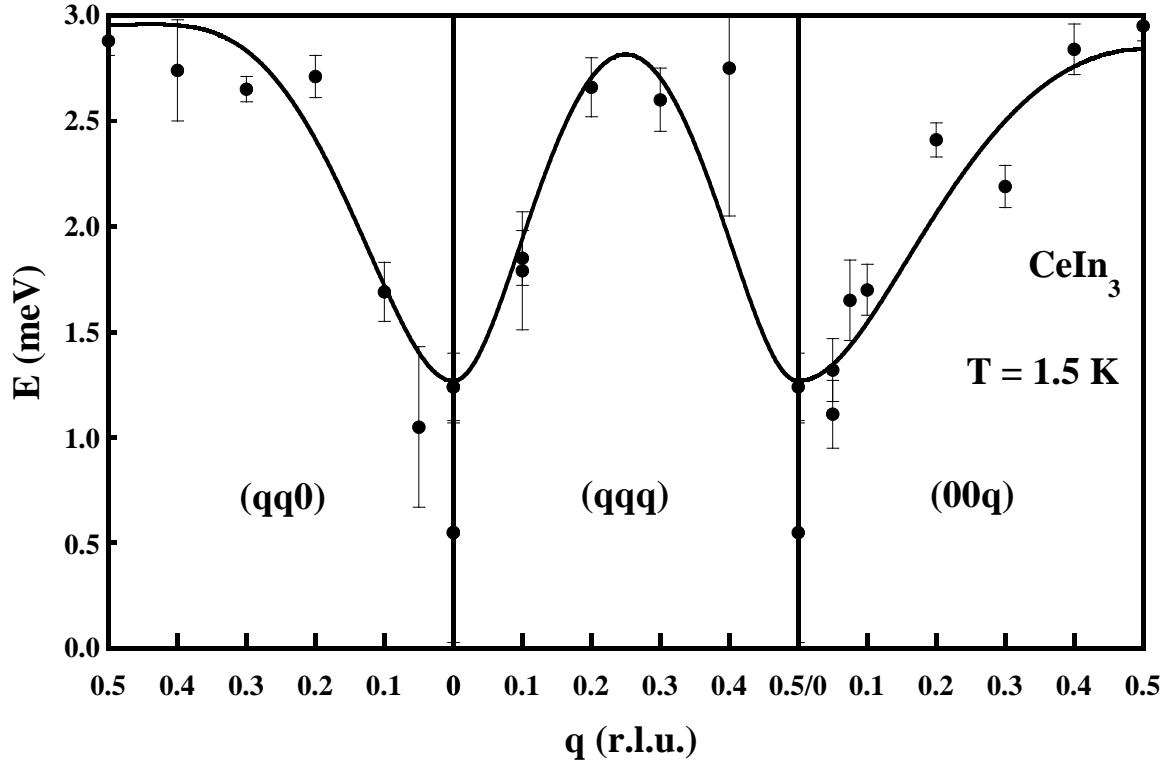


Figure 4. Spin-wave dispersion of $CeIn_3$ along the three main directions $(0,0,q)$, $(q,q,0)$ and (q,q,q) at $T = 1.5$ K, obtained on the IN22 spectrometer using a final energy of 14.7 meV. The solid line is a fit obtained using the molecular-field random-phase approximation.